

Measurement of Viscosity of SiO₂-CaO-Al₂O₃ Slag in Wide Temperature Range by Aerodynamic Levitation and Rotating Bob Methods and Sources of Systematic Error

Dimitrios SIAFAKAS¹, Taishi MATSUSHITA¹, Shinya HAKAMADA², Kenta ONODERA², Florian KARGL³, Anders E. W. JARFORS¹ and Masahito WATANABE²

Abstract

Viscosity measurements for SiO₂-CaO-Al₂O₃ based ternary slags with low SiO₂ content were performed for a wide temperature range utilizing the aerodynamic levitation and rotating bob methods. Aerodynamic levitation was used for temperatures ≥ 2229 K and the viscosity was calculated by the sample oscillation decay time. The rotating bob method was used for temperatures ≤ 1898 K and the viscosity was determined by the variation of the torque at different rotation speeds. Fitting curves were created using Mauro's viscosity equation. The main sources of systematic error were identified to be the sample weight measurement, the resolution of the high-speed camera, the fitting of the linear trend line in the torque against rpm diagrams and the vertical position of the bob. The combined standard uncertainty from all error sources was calculated for both measurement methods.

Keyword(s): Aerodynamic levitation, Slag, Viscosity, Rotating bob, Gravity

Received 26 February 2018, Accepted 16 April 2018, Published 30 April 2018.

1 Introduction

Accurate simulation related to metallurgical process requires input in the form of reliable and accurate thermophysical properties such as viscosity, density, and surface/interfacial tension. Deep understanding of interfacial phenomena between molten slag and molten steel is essential to be able to optimize iron and steelmaking processes. The generation of reliable thermophysical data poses a serious scientific challenge. Accurate measurements are extremely difficult due to reactions with crucible walls or other containing surfaces. The situation with respect to the viscosity of liquid oxide or slag is similar. In this respect, containerless measurements technique provides a promising route towards obtaining reliable thermophysical properties data. The containerless measurement technique is a promising way to obtain reliable thermophysical properties at elevated temperatures as the contamination from surroundings (e.g. container) can be minimized and the temperature can be elevated to higher values compared to measurements with container as there is no restriction by container material.

Using a containerless technique for viscosity measurements of liquid oxides, the surface oscillating method should be applied to obtain the viscous damping time. However, to obtain the viscous damping time the electrostatic levitation (ESL) technique has to be applied¹). However, since ESL requires an ultrahigh vacuum to avoid sparking at the electrode, the types of

samples that can be used with this system on the ground are limited due to their evaporation rate in a vacuum. The density, surface tension and viscosity of molten Al₂O₃ can be measured using ESL because of its low evaporation rate in a vacuum. However, the high vacuum evaporation rates of other oxide materials make measuring the thermophysical properties of their melts difficult in the ESL technique on the ground. To avoid the fore mentioned problem the thermophysical properties of a molten slag composed of SiO₂-CaO-Al₂O₃, which readily evaporates in a vacuum, can be measured using the electrostatic levitation furnace (ELF) facility on the "KIBO" module of the International Space Station (ISS). The microgravity conditions on the ISS negate the need for a high vacuum in ESL as the sample can be levitated using a very small electrostatic force. Due to the limited time allocated on the ISS, it will only be possible to conduct interfacial tension measurements between liquid iron and molten slags. However, to analyze the interfacial tension measurements acquired on the ISS, accurate viscosity values of the slag are required. To obtain the required viscosity values, a ground based, containerless technique that overcomes the evaporation problems had to be developed. The aerodynamic levitation (ADL)²), with surface oscillation technique was utilized for the measurements. To generate surface oscillations on the levitated droplet, Langstaff *et al.*²) invented the acoustic excitation method using audio speakers. It was confirmed that the generation of the normal mode of the

1 Department of Materials and Manufacturing, Jönköping University, 55111 Jönköping, Sweden.

2 Department of Physics, Gakushuin University, 1-5-1 Mejiro, Tokyo, 171-8588 Japan.

3 Institute of Materials Physics in Space, German Aerospace Center (DLR), 51170 Cologne, Germany.
(E-mail: dimitrios.siafakas@ju.se)

natural surface oscillation in the levitated droplet can also be obtained by the acoustic excitation method to the gas-jet flow²⁾. The normal mode of the natural surface oscillations of the levitated droplet, which is analyzed by Rayleigh³⁾ and by Lamb⁴⁾, is very important for the surface tension and viscosity measurements using the surface oscillation method. By these confirmations, it was certified that viscosity and surface tension can be obtained by this method on the ground⁵⁾. For viscosity below 100 mPa·s, a viscosity value can be obtained by the surface oscillation method but for viscosity higher than 100 mPa·s it becomes difficult to generate surface oscillation with enough amplitude to measure the viscosity. The viscosity of liquid oxide largely varies from about 1 Pa·s to 10 mPa·s depending on the temperature, and thus the surface oscillation method (ADL technique) cannot be applied for the measurement of the lower viscosity range of molten slag.

In this study, to obtain viscosity in the wider temperature range for molten slag, in addition to the surface oscillation method with ADL system for the higher temperature range, the rotating bob method was applied for the lower temperature range (i.e. lower viscosity range). In addition to the measurement at a lower temperature range, the rotating bob method, also, allows the viscosity measurement of suspension, and thus the measurement in the solid-liquid coexistence zone is possible. In the lower temperature region, the reaction between liquid oxides and container materials is not significant and the viscosity measurements should not be affected by the contamination.

In this study, the viscosity of SiO₂-CaO-Al₂O₃ system was measured in a wide temperature range (1623 K – 2800 K) using ADL and rotating bob methods. The viscosity of SiO₂-CaO-Al₂O₃ system has been investigated by many groups and the influence of the silicate network and cation effect on the viscosity is well-known⁶⁾. However, the viscosity of low silica SiO₂-CaO-Al₂O₃ has not been explored so much. The current study aims to validate if the ADL and rotational bob methods can be considered as good alternatives to acquire accurate viscosity values in normal gravity conditions, check if any of

the known models that describe viscosity is applicable and to identify the main sources of systematic error. The compositional dependence of the viscosity of low-SiO₂-CaO-Al₂O₃ slag systems is out of the scope of the present paper and will be published as a separate paper in the future.

2 Experimental

2.1 Materials

The viscosity of six different ternary slag systems containing SiO₂, Al₂O₃ and CaO were measured. The compositions, liquidus and solidus temperatures, and basicity (CaO/(SiO₂+Al₂O₃) in mass % of each slag system are shown in **Table 1**. The liquidus and solidus temperatures were calculated with Thermo-Calc software SLAG3.2 database⁷⁾. The basicity was defined as the value of CaO / (SiO₂+Al₂O₃) (mass% ratio) since in the present slag systems, the amphoteric oxide, Al₂O₃, acts as a network former⁸⁾.

2.2 Procedure

2.2.1 Rotating Bob Method

Viscosity measurements for lower temperature zone (1623 K – 1898 K) were performed by the rotating bob method with a Brookfield digital viscometer (DV2T-LV, maximum torque: 7.187×10⁻⁴ Nm). **Figure 1** shows a schematic illustration of the experimental setup and detailed designs of the molybdenum spindle and BN crucible.

The SiO₂, (Sigma-Aldrich, – 325 mesh, 99.5% trace metal basis) Al₂O₃ (Sigma-Aldrich, α-phase, –100 mesh, 99%) and CaO powders were mixed using a mortar and a muller to obtain the desired slag composition. The mixed powders were compressed into a BN crucible. CaO was produced by heating up CaCO₃ powder (Sigma-Aldrich, ACS reagent, ≥99%) to 1223 K for 12 hours in a muffle furnace.

The mixed powders were heated up to 1873 K or 1923 K with a rate of 10 K min⁻¹ under Ar atmosphere for complete melting, kept at this temperature for 20 minutes to homogenize and then cooled to the target temperature at a rate of 10 K·min⁻¹. Before

Table 1 Compositions, liquidus/solidus temperatures and basicity of slag systems (mass%).

Slag No.	SiO ₂	Al ₂ O ₃	CaO	Liquidus temp.[K] (Thermo-Calc)	Solidus temp.[K] (Thermo-Calc)	Basicity CaO/(SiO ₂ +Al ₂ O ₃)
1	10	40	50	1681	1614	1.00
2	10	35	55	1639	1613	1.22
3	10	30	60	1773	1637	1.50
4	14	36	50	1665	1616	1.00
5	10	44	46	1722	1620	0.85
6	20	30	50	1792	1668	1.00

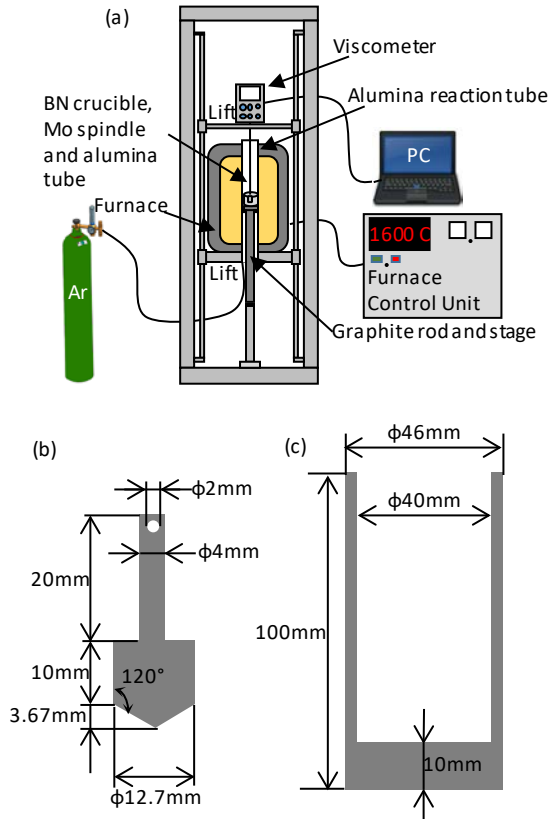


Fig. 1 (a) Schematic illustration of experimental setup, (b) molybdenum spindle and (c) BN crucible.

starting the measurement, the spindle was immersed into slag and lowered to the desired height. The spindle was suspended by a dense Al_2O_3 rod and molybdenum wire and the tip was positioned 15 mm below the slag meniscus. All viscosity measurements were performed during the cooling cycle at temperature increments of 25 or 50 K.

After steady state was confirmed at each temperature by allowing the spindle to rotate until the torque value was

stabilized, the torque was measured for 120 seconds and logged every second using a data logger. The rotation speed varied between 3 RPM and 120 RPM and the measurements were repeated for 3 to 7 different rotation speeds depending on the torque limitation of the viscometer. The viscosity was calculated from the slope of the rotation speed and torque. The torque at each rotation speed was determined as the average value of all 120 samplings.

The calibration of the viscometer was performed using standard silicone oils (97, 494 and 985 mPa·s) at 298 K at various rotation speeds. Though, at elevated temperatures, the diameter of the molybdenum bob will be increased due to the thermal expansion, leading to an overall increase in the value of the torque. In the present study, to compensate for the change of the torque due to thermal expansion, the diameter of the bob at each temperature was estimated by **Eq. 1**, which describes the thermal expansion of molybdenum⁹⁾.

$$\begin{aligned} \Delta L/L_0 = & 0.760 + 7.583 \cdot 10^{-4}(T - 1545) \\ & + 1.329 \cdot 10^{-7}(T - 1545)^2 \\ & + 1.149 \cdot 10^{-10}(T - 1545)^3 \end{aligned} \quad (1)$$

(1545 K < T < 2800 K)

Then, the influence of the diameter change on the torque was estimated using a multiphysics simulation software, COMSOL Multiphysics® software. The model was structured based on the Fluid Flow (laminar flow) and Structural Mechanics (solid mechanics) modules of the software. The geometry was designed to represent the bob shown in **Fig. 1(b)** and the dimensions of the shaft and bob parts were changed according to the calculated thermal expansion. The equations to calculate the viscosity at each temperature are shown in **Table 2**.

2.2.2 ADL Method

For the higher temperature zone (2229 – 2800 K), the measurements were performed by the ADL incorporating a surface oscillation excitation system. The ADL technique is a containerless method where a sample is floated in a fixed position using a gas jet flow generated from conical nozzles. **Figure 2** shows a schematic illustration of the experimental setup.

Spherical solid oxide samples of about 2mm in diameter were levitated in the gas-jet flow and then melted under container-less conditions by CO_2 lasers which irradiated the samples from the top and bottom directions. The sample temperature was measured using a monochromatic pyrometer at a wavelength of 1.45 μm . To induce surface oscillations in the ADL droplet, the acoustic oscillation method was applied. Two phase-matched audio speakers were placed in a small chamber and inserted into the gas flow path between the mass-flow controller and the conical nozzle. A single-wavelength signal was applied to the speakers. The generated surface oscillations

Table 2 Viscosity equation per temperature.

Temperature [K]	Viscosity, η [Pa·s]
1898	$\eta = 0.6583a - 0.00612$
1873	$\eta = 0.6589a - 0.00509$
1823	$\eta = 0.6602a - 0.00513$
1773	$\eta = 0.6613a - 0.00510$
1723	$\eta = 0.6623a - 0.00513$
1698	$\eta = 0.6627a - 0.00511$
1673	$\eta = 0.6632a - 0.00513$
1648	$\eta = 0.6638a - 0.00514$
1623	$\eta = 0.6643a - 0.00515$

* The a in the equations is the slope of the linear trendline of the rotation speed against torque diagram

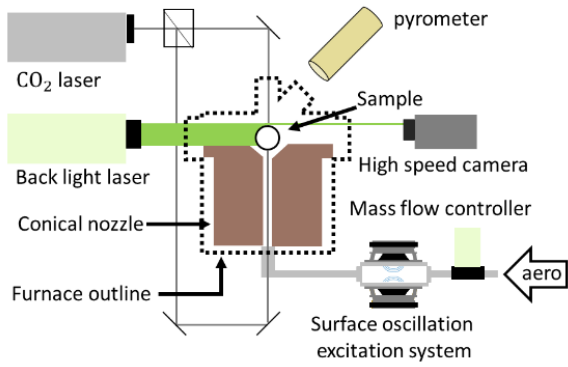


Fig. 2 Schematic illustration of ADL apparatus.

were observed using a high-speed camera that recorded the shadows produced by a 539nm backlight laser system, which reduced the effects of radiation from the molten oxide.

The shape of an undeformed levitated droplet is described by **Eq. 2** using spherical harmonics, Y_l^m and the time dependent radius r :

$$r(\theta, \varphi, t) = R + a(t)Y_l^m(\theta, \varphi) \quad (2)$$

where R is the radius of an undeformed sphere. The time dependent radius, r , depends also on the polar and azimuthal angles, θ and φ , respectively. $a(t)$ shows the time dependent deformation, l and m are integers characterizing the oscillation mode.)

According to Rayleigh⁴⁾, the normal mode frequency of the natural surface oscillation is described by **Eq. 3**

$$\omega_{l,m}^2 = l(l+2)(l-1) \frac{\sigma}{\rho R^3} \quad (3)$$

where σ , ρ , R are the surface tension, density and undeformed radius of the droplet, respectively.

The frequencies described in **Eq. 3** do not depend on the oscillation mode index m for small deformations. The ADL droplet can be assumed to be an undeformed sphere when no external acoustic excitation of oscillation is applied. For the surface tension measurements, the fundamental mode of $l = 2$ is important. $l = 2$ mode is a five-fold degenerate and considered as the lowest possible surface mode. Therefore, the fundamental mode frequencies for the natural surface oscillation, $\omega_{2,0}$, or Rayleigh frequencies, can be described as,

$$\omega_{l,m}^2 = \frac{8\sigma}{\rho R^3} \quad (4)$$

When the normal mode frequencies are input into the acoustic oscillation system, the sample resonates at an $l=2$, $m=0$ oscillation mode. After the signal generation is stopped, the

sample continues to oscillate in the same oscillation mode, but the amplitude decreases exponentially.

Viscosity, η , can then be obtained from the amplitude decay time constant, τ , of the fundamental mode $l=2$ in the case of natural surface oscillation by **Eq. 5**⁴⁾.

$$\eta = \frac{\rho R^2}{5\tau} \quad (5)$$

For high temperature – low viscosity conditions where the decay time is long, the decay time constant, τ can be obtained from a dumping sine curve described by **Eq. 6**⁵⁾.

$$a(t) = R_0 + R \sin(\omega_R t) \exp\left(-\frac{t}{\tau}\right) \quad (6)$$

where R_0 is the initial sphere radius and τ is the decay time constant.

However, in low temperature – high viscosity conditions **Eq. 6** cannot be used because the decay time is correspondingly short and large errors are observed when the experimental oscillation data is fitted in the curve.

3 Results

The results of the viscosity measurements of Slag 1 to Slag 6 at different temperatures are shown in **Fig. 3**. The results in solid-liquid coexistence zone (i.e. between solidus and liquidus temperatures) are denoted by the blue dots.

The fitting for the measured viscosity values against temperature was done by using Mauro's equation¹⁰⁾.

$$\log_{10} \eta = \log_{10} \eta_{\infty} + \frac{K}{T} \exp\left(\frac{C}{T}\right) \quad (7)$$

where η is the viscosity, T is the temperature, η_{∞} is the fitting parameter which corresponds to the viscosity at infinite temperature, K is the fitting parameter which is related to effective activation barrier and configurational entropy and C is the fitting parameter which is related to topological degrees of freedom per atom¹¹⁾.

For the curve fitting, only the experimental data for fully molten slags was used. Towards the lower temperature side, the curves were extrapolated (dashed line) and thus represent the viscosity value that the slag should have if no solid existed. The fitting parameters are summarized in **Table 3**.

Usually, the viscosity values in the solid-liquid coexistence zone deviate to higher values than those values predicted from the viscosity of fully molten state. Though, in the case of the present study it was observed that the experimental data fits the projection well which indicates that the influence of the solid phase on the viscosity was minimal. An unusual deviation from the projected fitting values towards lower viscosities was

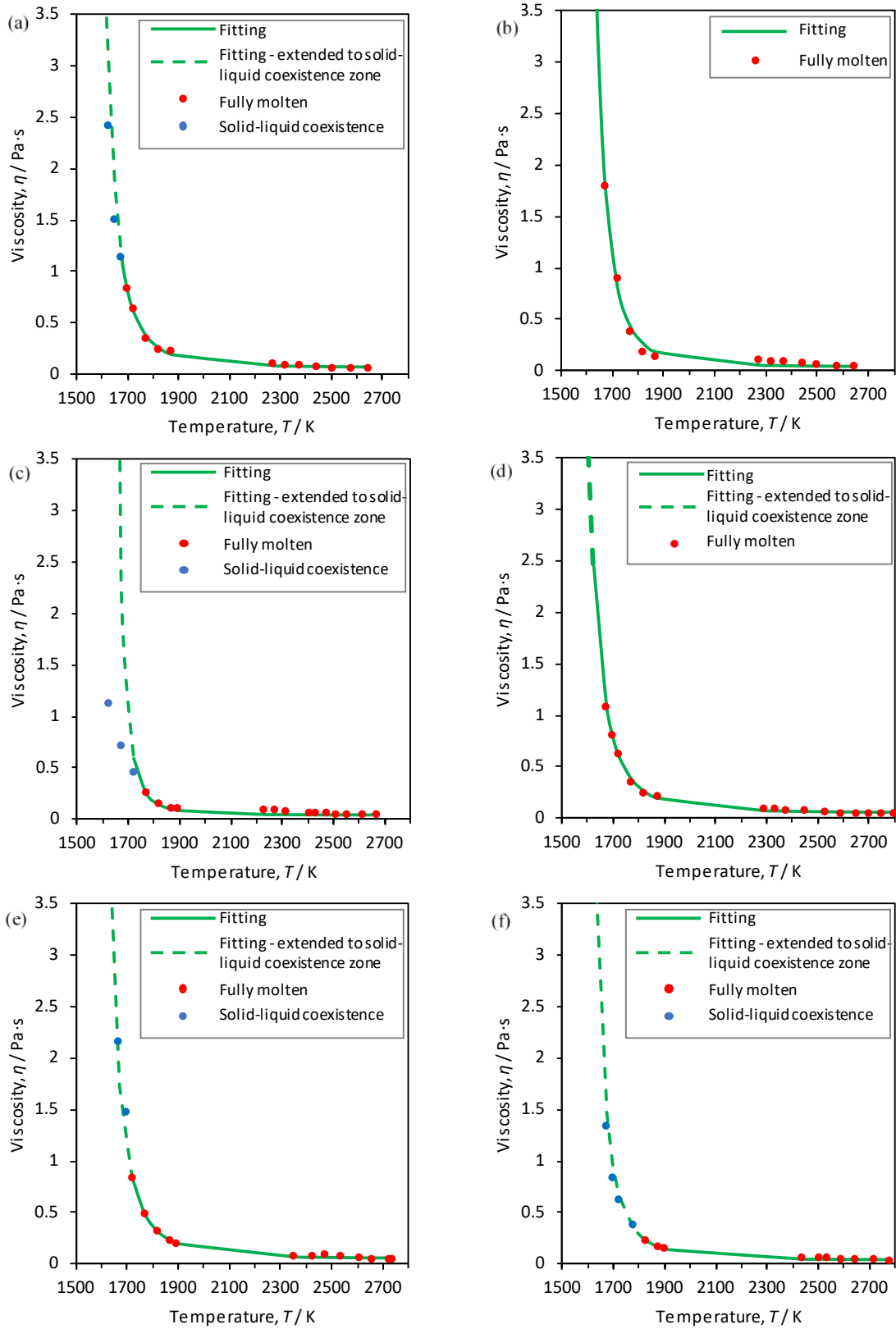


Fig. 3 Viscosity against temperature diagrams for (a) Slag 1, (b) Slag 2, (c) Slag 3, (d) Slag 4, (e) Slag 5 and (f) Slag 6.

Table 3 Parameters in the Mauro equation.

	Slag 1	Slag 2	Slag 3	Slag 4	Slag 5	Slag 6
$\log_{10}\eta_{\infty}$	-1.2406	-1.4778	-1.3346	-1.3215	-1.3102	-1.3793
K	1.0534	2.6256	0.005289	3.4621	2.6216	1.0622
C	12794	11725	21982	10853	11537	13056

observed in the solid-liquid coexistence zone for Slag 3 (**Fig 3(c)**). Considering that the fitting was performed using only the data from fully molten slag and the fact that Slag 3 starts to solidify at low viscosity values (approx. 250 mPa·s), the deviation can be attributed to the lack of sufficient data points at the region where the viscosity exponentially raised. Thus, the extrapolation of the curve resulted in the overestimation of the viscosity.

4 Discussion

4.1 Assessments of the Measurement Error (Rotating Bob Method)

The systematic error of the measurement was estimated based on the measurable error factors. The major error factors are the fitting of the linear trend line in the torque against rpm diagrams and the vertical position of the molybdenum bob, that is, the immersed depth of the bob.

The viscosity was obtained from the slope of the fitting line of the torque against RPM graph, a . However, the R2 values were not 1. This implies that there is an error in the slope a . The measurement error (standard deviation) of the slope was calculated based on the linear regression for each measurement.

The standard deviation of the viscosity due to the error of the slope of torque against RPM graph, σ_{fitting} , can be given **Eq. 8**.

$$\sigma_{\text{fitting}} = (b_{\eta}) \cdot (\sigma_a) \quad (8)$$

where b_{η} is the coefficient for the viscosity equation in **Table 2**

and σ_a is the standard deviation of the slope of the fitting line of the torque against RPM graph, a .

Apart from the error caused by the above-mentioned fitting error, the torque value will be influenced by the immersed depth. The top lift of the experimental setup allowed to control the vertical position of the bob with an accuracy of ± 0.5 mm. The ± 0.5 mm uncertainty in the vertical position is directly connected with a corresponding change in the total volume of the bob that is submerged in the molten slag and, thus, can influence the measured value of torque. The relative change of the torque due to the uncertainty of the vertical position of the bob was calculated using the same COMSOL model as for the thermal expansion, mentioned in the experimental section, by changing the geometry. It was found that the relative torque change due to the bob height error is ± 2.25 %. The standard deviation of the viscosity due to the error of the bob height, σ_{height} , can be given by **Eq. 9**.

$$\sigma_{\text{height}} = 0.0225a \cdot (b_{\eta}) \quad (9)$$

where a is the slope of the fitting line of the torque against RPM graph.

Assuming direct measurement error, the combined standard uncertainty of the viscosity measurement, σ_{total} , can be described by **Eq. 10**.

$$\sigma_{\text{total}} = \sqrt{(\sigma_{\text{fitting}})^2 + (\sigma_{\text{height}})^2} \quad (10)$$

Table 4 Combined standard uncertainty for the rotational bob method.

Temperature [K]	Slag 1	Slag 2	Slag 3	Slag 4	Slag 5	Slag 6
	Viscosity [Pa·s]					
1898	-	-	0.089±0.002	-	0.195±0.006	0.149±0.004
1873	0.215±0.008	0.129±0.005	0.091±0.002	0.203±0.007	0.223±0.006	0.167±0.004
1823	0.241±0.006	0.184±0.005	0.148±0.004	0.238±0.006	0.309±0.007	0.230±0.005
1773	0.349±0.009	0.382±0.009	0.249±0.006	0.352±0.008	0.481±0.011	0.370±0.009
1723	0.629±0.016	0.898±0.028	0.449±0.016	0.625±0.016	0.833±0.021	0.624±0.014
1698	0.830±0.020	-	-	0.805±0.019	1.476±0.036	0.835±0.020
1673	1.135±0.027	1.794±0.055	0.707±0.016	1.081±0.025	2.149±0.049	1.342±0.031
1648	1.502±0.040	-	-	-	-	-
1623	2.418±0.058	-	1.108±0.027	-	4.415±0.099	-

Table 5 Combined standard uncertainty for the ADL method.

Temperature [K]	Slag 1 Viscosity [mPa·s]	Temperature [K]	Slag 2 Viscosity [mPa·s]	Temperature [K]	Slag 3 Viscosity [mPa·s]
2273	107.0±17.5	2229	77.5±9.8	2230	77.2±10.2
2323	83.4±10.6	2287	69.0±7.8	2272	77.2±10.2
2373	84.5±10.9	2313	68.1±7.6	2317	61.2±6.4
2443	66.9±6.9	2375	67.7±7.5	2408	51.3±4.5
2503	54.1±4.9	2450	52.6±4.6	2435	45.0±3.5
2579	46.3±3.3	2488	47.5±3.7	2474	43.6±3.3
2647	46.4±3.3	2592	41.9±2.9	2510	37.7±2.5
		2643	39.4±2.7	2558	39.5±2.7
		2683	39.4±2.7	2615	35.1±2.1
		2723	38.6±2.6	2674	35.1±2.1

Temperature [K]	Slag 4 Viscosity [mPa·s]	Temperature [K]	Slag 5 Viscosity [mPa·s]	Temperature [K]	Slag 6 Viscosity [mPa·s]
2289	92.8±12.5	2355	78.6±11.3	2435	64.5±6.6
2332	88.9±11.5	2430	77.8±11.0	2502	58.4±5.4
2378	79.4±9.2	2478	91.2±15.1	2534	53.9±4.6
2448	66.3±6.4	2536	69.1±8.7	2591	47.0±3.6
2530	53.6±4.2	2611	51.8±4.9	2643	44.4±3.2
2591	47.5±3.3	2662	42.6±3.3	2718	40.2±2.6
2653	42.1±2.6	2726	44.7±3.7	2780	32.5±1.8
2701	38.2±2.1	2741	40.0±2.9		
2749	37.0±2.0				
2800	37.0±2.0				

The combined standard uncertainties at each data point are summarized in **Table 4**.

4.2 Assessments of the Measurement Error (ADL Method)

The measurement error of the droplet oscillation method by the aerodynamic levitation comes from the resolution of the camera and the accuracy of the weight measurement. The time resolution of the camera was 1000 FPS and the spatial resolution was 5.3×10^{-3} mm / pixel.

The viscosity was obtained from the radius of the sample and the decay time of oscillation. To obtain an accurate radius value is very difficult because the radius of the sample is measured in pixel units in the camera image. The sample radius had an uncertainty of $\pm 5.3 \times 10^{-3}$ mm. The uncertainty of viscosity due to the uncertainty of radius value was obtained by the sensitivity coefficient described in **Eq. 11**.

$$\sigma_{\text{radius}} = \frac{\partial \eta}{\partial R} \cdot \Delta R \quad (11)$$

where $\frac{\partial \eta}{\partial R}$ is the partial derivative of **Eq. 5** with respect to the mass and ΔR is the uncertainty of radius R .

The decay time of surface oscillation was obtained from the sample diameter variation with time. Camera recording rate was 1000 frame per second. Measurement of decay time constant had an accuracy of 1.0×10^{-3} sec. The uncertainty of viscosity due to the accuracy of the decay time constant can be described by **Eq. 12**.

$$\sigma_{\text{decay time}} = \frac{\partial \eta}{\partial \tau} \cdot \Delta \tau \quad (12)$$

where $\frac{\partial \eta}{\partial \tau}$ is the partial derivative of **Eq. 5** with respect to the mass and $\Delta \tau$ is the uncertainty of decay time constant τ .

The density in **Eq. 5** was obtained from the volume calculated from the image and the mass measured before floating. The mass was weighed three times per sample, the average was calculated, and the uncertainty was obtained from a scatter. The uncertainty of viscosity due to the accuracy of mass can be described by **Eq. 13**.

$$\sigma_{\text{mass}} = \frac{\partial \eta}{\partial m} \cdot \Delta m \quad (13)$$

where, $\frac{\partial \eta}{\partial m}$ is the partial derivative of Eq. 5 with respect to the mass and Δm is the uncertainty of mass.

Volume uncertainty was calculated by including it in the above uncertainty of the radius.

Assuming direct measurement error, the combined standard uncertainty of the viscosity measurement, σ_{total} , can be described by Eq. 14.

$$\sigma_{\text{total}} = \sqrt{(\sigma_{\text{radius}})^2 + (\sigma_{\text{decay time}})^2 + (\sigma_{\text{mass}})^2} \quad (14)$$

The combined standard uncertainties at each data point are summarized in Table 5.

5 Conclusions

In this study, the viscosity of SiO₂-CaO-Al₂O₃ based slags with low SiO₂ content was determined for a wide range of temperatures (1623 K – 2800 K) under normal gravity condition utilizing the rotating bob and ADL methods. It was found that the experimental data can be described using Mauro's equation in a wide temperature range. The sources of systematic error were determined, and the combined standard uncertainties were assessed for both measurement methods. In such a way, accurate viscosity values were obtained that can later be used

for the analysis of the interfacial tension measurements obtained on the ISS.

Acknowledgments

This research was supported by JAXA, the MEXT-Support Program for the Strategic Research Foundation at Private Universities, 2015-2019 and partially funded by the Swedish National Space Board. We appreciate their support.

References

- 1) P.F. Paradis and T. Ishikawa: Japanese journal of applied physics, **44** (7R) (2005) 5082.
- 2) D. Langstaff, M. Gunn, G.N. Greaves, A. Marsing and F. Kargl, : Review of Scientific Instruments, **84** (12) (2013) 124901.
- 3) H. Lamb: Proceedings of the London Mathematical Society, 1, London, Great Britain (1881) 51.
- 4) L. Rayleigh: Proc. R. Soc. London, **29**, London, Great Britain, January (1879) 71.
- 5) S. Hakamada, A. Nakamura, M. Watanabe and F. Kargl: Int. J. of Microgravity Science and Application, **34** (2017) 340403.
- 6) P. Kozakevitch and T.G. John: J. of The Minerals, Metals & Materials Society, **21** (7) (1969) 57.
- 7) J. Andersson, T. Helander, L. Höglund, P. Shi and B. Sundman: Calphad, **26** (2) (2002) 273.
- 8) J.H. Park, D.J. Min and H.S. Song: Metallurgical and Materials Transactions B, **35** (2) (2004) 269.
- 9) Y.S. Touloukian, S.C. Saxena and P. Hestermans: Thermophysical Properties of Matter-the TPRC Data Series, **11** (Viscosity) (1975).
- 10) S.C. Waterton: J. Soc. Glass Technol, **16** (1932) 244.
- 11) J.C. Phillips: Non-Cryst. Solids, **34** (1979) 153.